Structural and Biochemical Characterization of Toad Liver Fatty Acid-Binding Protein[†,‡]

Santiago M. Di Pietro,*[,§] Betina Córsico,[#] Massimiliano Perduca,[⊥] Hugo L. Monaco,[⊥] and José A. Santomé[§]

Instituto de Química y Fisicoquímica Biológicas (IQUIFIB)-CONICET-UBA, Facultad de Farmacia y Bioquímica, UBA, Junín 956, Buenos Aires 1113, Argentina, Instituto de Investigaciones Bioquímicas de La Plata (INIBIOLP)-CONICET-UNLP, Facultad de Ciencias Médicas, UNLP, Calle 60 y 120, La Plata 1900, Argentina, and Laboratorio di Biocristallografia, Dipartimento Scientifico e Tecnologico, Università di Verona, Strada Le Grazie 15, 37134 Verona, Italy

Received February 6, 2003; Revised Manuscript Received May 12, 2003

ABSTRACT: Two paralogous groups of fatty acid-binding proteins (FABPs) have been described in vertebrate liver: liver FABP (L-FABP) type, extensively characterized in mammals, and liver basic FABP (Lb-FABP) found in fish, amphibians, reptiles, and birds. We describe here the toad Lb-FABP complete amino acid sequence, its X-ray structure to 2.5 Å resolution, ligand-binding properties, and mechanism of fatty acid transfer to phospholipid membranes. Alignment of the amino acid sequence of toad Lb-FABP with known L-FABPs and Lb-FABPs shows that it is more closely related to the other Lb-FABPs. Toad Lb-FABP conserves the 12 characteristic residues present in all Lb-FABPs and absent in L-FABPs and presents the canonical fold characteristic of all the members of this protein family. Eight out of the 12 conserved residues point to the lipid-binding cavity of the molecule. In contrast, most of the 25 L-FABP conserved residues are in clusters on the surface of the molecule. The helix−turn−helix motif shows both a negative and positive electrostatic potential surface as in rat L-FABP, and in contrast with the other FABP types. The mechanism of anthroyloxy-labeled fatty acids transfer from Lb-FABP to phospholipid membranes occurs by a diffusion-mediated process, as previously shown for L-FABP, but the rate of transfer is 1 order of magnitude faster. Toad Lb-FABP can bind two *cis*-parinaric acid molecules but only one *trans*-parinaric acid molecule while L-FABP binds two molecules of both parinaric acid isomers. Although toad Lb-FABP shares with L-FABP a broad ligand-binding specificity, the relative affinity is different.

Cytosolic fatty acid-binding proteins (FABPs)[1] belong to a multigene family of intracellular proteins which are named according to the first tissue they were isolated from. A very high sequence conservation has been shown to exist between FABPs isolated from the same tissue in different species (*1*−*4*), whereas the different FABP types in one species show amino acid sequence identities ranging from 20 to 70% (*3*, *4*). The primary structures of liver FABPs (L-FABPs) from the four mammalian species reported: rat, human, cow, and pig display a 79−90% amino acid identity with one another (*4*). On the other hand, the amino acid sequence of a basic FABP (pI 9.0) from chicken liver (Lb-FABP) showed an amino acid identity between 28 and 43% with the other members of the family (*5*). According to these results and to an evolutionary analysis based on the primary structure (*6*), chicken Lb-FABP was the first nonmammalian FABP reported to belong to the liver FABP subfamily. However, the amino acid identity percentages between chicken Lb-FABP and mammalian L-FABPs are rather low for FABPs of the same type and chicken Lb-FABP was suggested to represent a new type of FABP different from those already known (*4*−*8*). More recently, a number of liver FABPs related to chicken Lb-FABP were found in the liver of several

[†] S.M.D. acknowledges the Research Student Grant 2000 of the International Union of Pure and Applied Biophysics. This work was supported by grants from the Universidad de Buenos Aires and Consejo Nacional de Investigaciones Científicas y Técnicas de la República Argentina. B.C. acknowledges the NIH Grant R03 TW01100-01. The Biocrystallography Laboratory of the University of Verona was funded by the Italian Ministry of the Universities and Scientific Research (MURST).

[‡] The amino acid sequence reported in this work has been deposited in the SWISS−PROT data bank under accession number P83409. Coordinates of the model have been deposited in the Protein Data Bank (entry 1P6P).

* To whom correspondence should be addressed. Present address: Department of Human Genetics, UCLA School of Medicine, Gonda Center, Room 6554B, Los Angeles, CA 90095-7088, USA. Phone: 310-206-2148. Fax: 310-794-5446. E-mail: sdipietro@mednet.ucla.edu.

[§] Instituto de Química y Fisicoquímica Biológicas (IQUIFIB)-CONICET-UBA.

[#] Instituto de Investigaciones Bioquímicas de La Plata (INIBIOLP)-CONICET-UNLP.

[⊥] Università di Verona.

[1] Abbreviations: A-FABP, adipocyte fatty acid-binding protein; AOFA, anthroyloxy-labeled fatty acid; 12AO, 12-(9-anthroyloxy)oleic acid; CL, bovine heart cardiolipin; B-FABP, brain fatty acid-binding protein; PS, brain phosphatidylserine; CCP4, Collaborative Computational Project Number 4; CRBP, cellular retinol-binding protein; EPC, egg phosphatidylcholine; E-FABP, epidermal fatty acid-binding protein; FABP, fatty acid-binding protein; H-FABP, heart fatty acid-binding protein; HPLC, high-performance liquid chromatography; Il-FABP, ileal fatty acid-binding protein; I-FABP, intestinal fatty acid-binding protein; L-FABP, liver fatty acid-binding protein; Lb-FABP, liver basic fatty acid-binding protein; My-FABP, myelin fatty acid-binding protein; NBD-PC, *N*-(7-nitro-2,1,3-benzoxadiazol-4-yl) egg phosphatidyl choline; rmsd, root-mean-square deviation; SUVs, small unilamellar vesicles; S-FABP, sperm fatty acid-binding protein; TBS, Tris-buffered saline; TFA, trifluoroacetic acid.

10.1021/bi034213n CCC: $25.00
Published on Web 06/17/2003

fish, amphibians, and reptiles (*9*−*18*). We have also shown that Lb- and L-FABP were originated by ancient gene duplication and that both types are expressed in catfish and axolotl (*10*, *13*).

Several facts indicate that L-FABP is structurally and functionally different from the other FABP types. L-FABP binds two fatty acids per molecule (*19*−*22*), whereas the other FABP types have a single fatty acid-binding site (*23*, *24*). There have been some reports of binding of endogenous hydrophobic ligands other than long chain fatty acids, such as prostaglandins, retinoids, and acyl-CoAs, to several FABPs; however, L-FABP has the broadest substrate specificity among FABPs studied (*1*−*4*, *25*−*28*). The mechanism of fatty acid transfer to membranes is different in L-FABP when compared to the other members of the FABP family. Studies with a fluorescent analogue of fatty acids showed that the transfer from L-FABP to membranes is consistent with an aqueous mediated mechanism, whereas, using the same experimental approach, results obtained for all other FABPs examined to date, including H-FABP, A-FABP, B-FABP, and I-FABP, are likely to involve transient collisional protein−membrane interactions (*29*−*37*). It has also been shown that the helix−turn−helix motif is essential for the electrostatic interactions involved in the collisional transfer mechanism of H-, A-, and I-FABP (*32*, *33*, *36*). All of these FABP types have a positive electrostatic potential contour in that molecular region which suggests that it is important for the interactions with the membranes (*38*). The presence of a both negative and positive electrostatic potential in the helix−turn−helix cap of L-FABP may be the cause preventing such an interaction (*38*).

Both Lb-FABP and L-FABP show a distinctive broad ligand-binding specificity and bind not only long chain-fatty acids but also other structurally different hydrophobic ligands (*1*−*4*, *13*, *14*, *18*, *25*−*28*). Differences regarding the binding capacity of these FABPs to *cis*- and/or *trans*-parinaric acid have been reported. Mammalian and axolotl L-FABP bind two *cis*- or *trans*-parinaric acid molecules per protein molecule (*13*, *22*, *23*), while axolotl, shark, and lungfish Lb-FABPs bind two *cis*-parinaric acid molecules but can accommodate only one *trans*-parinaric acid (*13*, *14*, *18*). Catfish Lb-FABP appears to bind only one *cis*- or *trans*-parinaric acid molecule (*10*) and chicken Lb-FABP binds only one ligand molecule (*8*, *39*).

To gain more knowledge on the structural and functional characteristics of Lb-FABPs and their relationship with L-FABP and other FABP types, we have extended our study of toad Lb-FABP whose isolation, partial amino acid sequencing, and crystallization we previously reported (*11*, *40*). We now describe its complete amino acid sequence, X-ray structure, ligand-binding properties, and mechanism of fatty acid transfer to phospholipid membranes.

EXPERIMENTAL PROCEDURES

Materials. Endoproteinases Glu-C and Lys-C were obtained from Promega and Chymotrypsin from Sigma. *cis*-Parinaric and *trans*-parinaric acids and the anthroyloxy-labeled fatty acid (AOFA), 12-(9-anthroyloxy)oleic acid (12AO) were from Molecular Probes, Inc. Egg phosphatidylcholine (EPC), *N*-(7-nitro-2,1,3-benzoxadiazol-4-yl) egg phosphatidyl choline (NBD-PC), brain phosphatidylserine (PS), and bovine heart cardiolipin (CL) were obtained from Avanti Polar Lipids. All other reagents were from Sigma, Baker, Bio-Rad, Pharmacia Biotech and/or Applied Biosystems.

Animals. Adult toads (*Bufo arenarum* var. Hensell) were collected in Buenos Aires, Argentina.

Toad Lb-FABP Purification and Delipidation. The 106 000*g* supernatant preparation and the protein purification were carried out as previously described (*11*). The purified Lb-FABP was delipidated by incubation, at 37 °C for 45 min, with Lipidex beads (*41*) before both parinaric acid binding and displacement assays and AOFA binding and transfer assays. To check the absence of residual endogenous ligands bound to the FABP after delipidation procedure, 70 nmol of the protein was lyophilized, dissolved in 0.5 mL of 8 M guanidine-HCl and lipids extracted as per Bligh and Dier (*42*). Lipids were determined by HPTLC using ethyl-acetate/isooctane/acetic acid/water (66:30:12:60) as the mobile phase and developed with iodine. Determination revealed that the FABP was essentially lipid-free with a detection limit of 4 pmol.

Pyridylethylation of the Protein. Toad Lb-FABP was pyridylethylated as described (*43*). The purified protein was incubated in 0.25 M Tris-HCl (pH 8.5), 6 M guanidine-HCl, 10 mM DTT, at 37 °C during 1 h. After reduction of the sample, the protein was alkylated by the addition of 2 μL of 4-vinylpiridine and incubation for 1 h at 37 °C. The sample was then desalted by HPLC (Pharmacia LKB) in a Vydac C_4 column (4.6 × 250 mm) equilibrated with solvent A [0.1% (v/v) TFA in water]. Elution was performed at a flow rate of 0.8 mL/min with a 0−100% linear gradient of solvent B [acetonitrile 80% (v/v), TFA 0.08% (v/v)] for 30 min.

Enzymatic Digestion and Peptide Purification. For Glu-C protease digestion, 200 μg of the pyridylethylated Lb-FABP was incubated in 0.1 M Tris-HCl (pH 7.9), 2 M urea, with 4 μg of enzyme, at 20 °C during 24 h. For Lys-C protease digestion, 150 μg of Lb-FABP was incubated in 0.1 M Tris-HCl (pH 8.5), 2 M urea, with 3 μg of enzyme, at 20 °C for 24 h. Peptides were separated by HPLC (Pharmacia LKB) in a Vydac C_{18} column (4.6 × 250 mm) equilibrated with solvent A [0.1% (v/v) TFA in water]. Elution was performed at a flow rate of 0.8 mL/min with a 0−80% linear gradient of solvent B [acetonitrile 80% (v/v), TFA 0.08% (v/v)] for 80 min. For chymotrypsin digestion, peak 3 of Lys-C digestion was lyophilized, dissolved, and incubated in 0.1 M Tris-HCl (pH 7.9), 2 M urea, with 1 μg of enzyme, at 20 °C, during 24 h. The resulting peptide mixture was fractionated by HPLC (Applied Biosystems) using a Brownlee Aquapore RP 300 C_{18} column (2.1 × 220 mm) equilibrated with solvent A and eluting at a flow rate of 0.17 mL/min with a 0−80% linear gradient of solvent B for 80 min.

Amino Acid Analysis and Sequence Determination. Quantitative amino acid analysis and automatic amino acid sequence determination by Edman degradation were carried out with an Applied Biosystems 420A Amino Acid Analyzer and an Applied Biosystems 477A Protein Sequencer, respectively, according to the manufacturer's instructions.

Sequence Alignment and Evolutionary Tree. Amino acid sequences were compared by using Multalin (http://pbil.ibcp.fr/cgi-bin/npsa_automat.pl?page=/NPSA/npsa-multalin.html) with a BLOSUM 62 matrix and default parameter values. The evolutionary tree was constructed with CLUSTAL W

(http:/www.ebi.ac.uk/clustalw/) by the Neighbor Joining method and applying the Kimura's distance correction procedure.

Crystal Structure Determination. The preparation of the single crystals of toad Lb-FABP has been described elsewhere (*40*). Diffraction data were collected at room temperature on a Rigaku R-axis II imaging plate area detector mounted on a Rigaku RU-200 rotating anode X-ray generator. The source was operated at 50 kV and 160 mA using a focal spot size of 0.3 × 3 mm. Monochromatic Cu Kα radiation was obtained using a graphite monochromator. The crystal-to-detector distance was 100 mm and the oscillation range 2°. Data indexing and integration were performed with the program Mosflm (*44*) and scaling and merging with the program Scala (*45*). The structure was solved using the CCP4 suite of programs for crystallographic computing (*45*). The initial phases were calculated using the molecular replacement method as implemented in the program AMoRe (*46*), with the coordinates of axolotl Lb-FABP (unpublished) as the search probe. When the rotation function was calculated with the data in the 8.0−3.5 Å resolution interval, it gave an unambiguous answer with a correlation coefficient of 21.2. The translation function was then calculated for all the space groups in class 422, and the best solution was found for space group $P4_322$; it had a correlation coefficient of 50.1, whereas the solution for space group $P4_122$ had a correlation coefficient of 34.4 which was not the second highest value found. Examination of the molecular packing in the unit cell after rigid body refinement showed that there were no clashings of the symmetry-related molecules in this space group and confirmed that the search model was indeed properly oriented and positioned in the cell. The initial model which had an R factor of 45.0 for the data up to 3.5 Å resolution was first rigid body refined moving initially the entire molecule and, in a second stage, the elements of secondary structure using the program TNT (*47*). After the proper side chains had been introduced, the model was subjected to a series of rounds of positional refinement alternated with manual model revisions using the program O (*48*) and the refinement program TNT. During the process of refinement and model building, the quality of the model was controlled using the program PROCHECK (*49*). Solvent molecules were added in the final stages of refinement according to hydrogen-bond criteria and only if their B factors refined to reasonable values and if they improved the Rfree. An Fobs − Fc map calculated with the final phases of the model does not show any features that could suggest a modification of the model but it has two significant peaks: an elongated electron density peak in the interior of the protein cavity that was not modeled using solvent molecules, and another corresponding to the acetyl group that must be present in the N terminus but was not included in the model. The final model contains 980 non-hydrogen protein atoms and has very reasonable geometry (see Table 1), with 86.5% of the residues in the most favored regions of the Ramachandran plot and the remaining 13.5% in the additionally allowed region. The R factor and rms deviations of Table 1 were calculated with the program TNT.

Surface Area and Electrostatic Potential Calculations. Surface area calculations were carried out using the program MSMS (*50*, *51*) with a probe sphere of 1.5 Å radius. The hydrogen atoms were added to the final PDB coordinates using the refinement program CNS (*52*) and the surface electrostatic potential was calculated with the program MEAD (*53*, *54*) using the default parameter values.

Table 1: Crystal Data Collection and Refinement Statistics of the Model[a]

space group	$P4_322$ (one molecule per asymmetric unit)
cell dimensions	$a = b = 48.140$ Å, $c = 135.230$ Å
resolution (Å)	20.0−2.5 (2.64−2.50)
total reflections	47,279
unique reflections	5917
overall completeness (%)	98.9 (98.9)
Rsym. (%)	6.4 (25.2)
multiplicity	8.0 (9.0)
$\langle I/\sigma(I)\rangle$	11.5 (3.0)
total reflections used	5827 (565)
reflections in working set	5266 (511)
reflections in test set	561 (54)
Rcryst. (%)	21.2 (26.9)
Rfree (%)	29.6 (31.0)
protein atoms	980
water molecules	25
rmsd on bond lengths, Å	0.006
rmsd on bond angles, °	1.413
rmsd on torsion angles, °	17.582

[a] Numbers in parentheses refer to the highest resolution shell.

Parinaric Acid-Binding Assay. These assays were performed as previously described (*10*, *13*, *18*, *22*, *23*, *27*, *28*). Two milliliter samples of toad Lb-FABP (1 μM) in 50 mM Tris-HCl (pH 7.4) were titrated with the addition of small increasing amounts of *cis*-parinaric or *trans*-parinaric acid up to a final concentration of 6.0 μM. The concentration of *cis*-parinaric and *trans*-parinaric acid stock solutions in ethanol (500 μM) was determined spectrophotometrically by using an ϵ_{308} value of 7.9×10^4 M^{-1} cm^{-1} and ϵ_{306} value of 7.7×10^4 M^{-1} cm^{-1}, respectively (*55*). Maximum fluorescence emission intensity (412 nm) caused by excitation at 324 nm was measured at 20 °C with a Jasco FP 770 spectrofluorometer with excitation and emission bandwidths of 3 nm. Data were corrected for blank fluorescence (ligand or protein only) and sample dilution, the latter never exceeding 1.5%. Ethanol concentration in the cuvette was under 1.5%.

Cis-Parinaric Acid Displacement Assay. Toad Lb-FABP (0.3 μM) in 50 mM Tris-HCl (pH 7.4) was incubated with *cis*-parinaric acid (1.0 μM) for 1 min and the maximum fluorescence intensity was recorded at 412 nm. Then, a 3-fold molar excess of displacing ligands was added from stock solutions in ethanol (except for acyl-CoAs, bezafibrate, and clofibrate, dissolved in 0.1 M sodium acetate, pH 6.0, and 10 mM NaOH, respectively), thoroughly mixed and allowed to equilibrate for 2 min before recording the fluorescence intensity again. Measurements were performed under the same conditions as above. Ethanol concentration after both *cis*-parinaric acid and competitor were added was under 2%.

Vesicle Preparation. Small unilamellar vesicles (SUVs) were prepared by sonication and ultracentrifugation (*56*, *57*). The standard vesicles were prepared to contain 90 mol % of EPC and 10 mol % of NBD-PC, which served as the fluorescence quencher. For some experiments, as indicated in the text, 25 mol % of other lipids was substituted for EPC in the vesicles. Vesicles were prepared in TBS (40 mM Tris, 100 mM NaCl, pH 7.4) except for SUVs containing CL which were prepared in TBS with 1 mM EDTA.

AOFA-Binding Assay. Binding of 12AO to toad Lb-FABP was determined with a fluoresce titration assay (*58*). Emission spectra of 12AO bound to the FABPs were obtained exciting at 383 nm.

Relative Partition Coefficient. The partition coefficient (*Kp*) for AOFA partitioning between toad Lb-FABP and SUVs was determined by measuring AOFA fluorescence at a given molar ratio of Lb-FABP:SUV after titration of SUV into a solution containing 5 μM Lb-FABP and 0.5 μM 12AO in TBS (*59*, *60*).

$$Kp = ([\text{Lb-FABP-bound AOFA}]/[\text{Lb-FABP}])/([\text{SUV-bound AOFA}]/[\text{SUV}])$$

The decrease in AOFA fluorescence upon titration of AOFA-containing Lb-FABP with SUVs was related to *Kp* by the following equation:

$$1/\Delta F = 1/Kp(1/\Delta F_{max})([\text{Lb-FABP}]/[\text{SUV}]) + 1/\Delta F_{max}$$

where ΔF is the difference between the initial fluorescence of AOFA in the Lb-FABP and the AOFA fluorescence at a given Lb-FABP/SUV ratio, and ΔF_{max} is the maximum difference in AOFA fluorescence. A plot of $1/\Delta F$ versus $(1/\Delta F_{max})([\text{Lb-FABP}]/[\text{SUV}])$ gives a slope of $1/Kp$. The partition coefficient was used to establish AOFA transfer assay conditions so as to ensure essentially unidirectional transfer, as described below (*61*).

Transfer of AOFA from FABPs to SUVs. A fluorescence resonance transfer assay was used to monitor the transfer of AOFA from toad Lb-FABP to acceptor model membranes as previously described (*33*). Briefly, FABP with bound AOFA was mixed with SUV using a Stopped-Flow Spectrofluorometer DX-17MV (Applied Photophysics Limited, UK). The NBD moiety is an energy transfer acceptor of the anthroyloxy group (AO) donor; therefore, the fluorescence of the AOFA is quenched when the ligand is bound to SUV containing NBD-PC. Upon mixing of the sample, transfer of AOFA from protein to membrane is directly monitored by the time-dependent decrease in AO fluorescence. Final transfer assay conditions were 12.5 μM Lb-FABP with 0.125 μM 12AO and 150 μM SUV. The AOFA binding constant was estimated using a fluorimetric titration as mentioned above. The toad Lb-FABP apparent K_D value for 12AO was 0.52 ± 0.03 μM. Thus, for the conditions used in the transfer experiment, we estimated that 96% of the AOFA is bound to Lb-FABP at time = 0. Determination of the relative partition coefficient for 12AO between Lb-FABP and PC-containing vesicles showed a preferential partitioning to Lb-FABP by a factor of approximately 7:1 (Lb-FABP/SUV). To ensure unidirectional transfer, experiments were performed under conditions where the acceptor-to-donor ratios (SUV/Lb-FABP) were above the equilibrium partition coefficient determined (*60*). Transfer was monitored at 25 °C. Controls to ensure that photobleaching was eliminated were performed prior to each experiment (*30*). Data were analyzed using software provided with the instrument, and all curves were well described by a single-exponential function. For each experimental condition, at least five replicates were carried out. Average values ± SD for three or more separate experiments are reported.

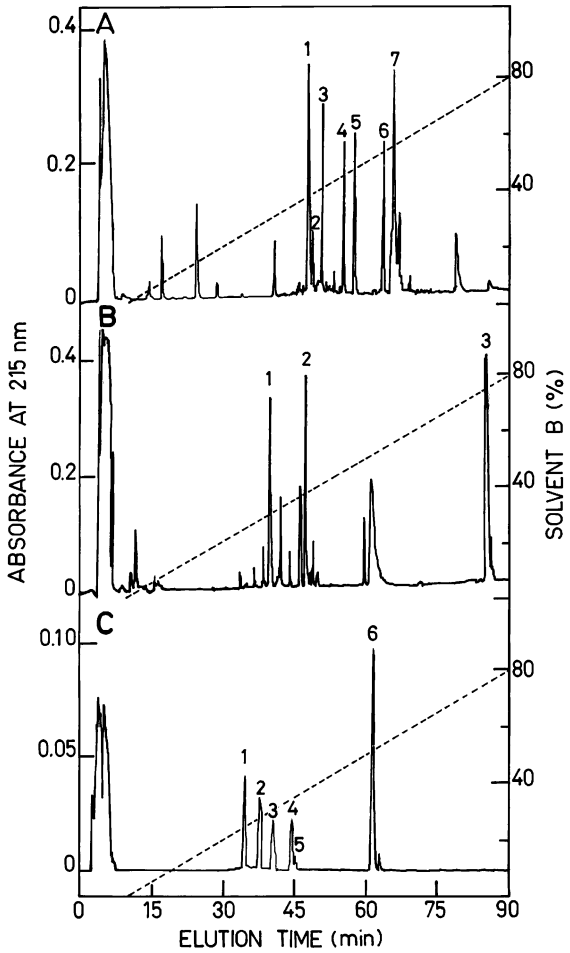

FIGURE 1: RP-HPLC separation of toad Lb-FABP peptides generated by enzymatic digestion. (A) The peptide mixture obtained by Glu-C digestion was separated in a Vydac C_{18} column (4.6 × 250 mm) equilibrated with solvent A [0.1% (v/v) TFA in water]. Elution was performed with a 0−80% linear gradient (dashed line) of solvent B [80% (v/v) acetonitrile, 0.08% (v/v) TFA]. (B) The products of Lys-C digestion were isolated as described for the Glu-C peptide mixture. (C) The peptide mixture obtained by chymotryptic digestion of N-terminal Lys-C peptide (K3) was fractionated in a Brownlee Aquapore RP 300 C_{18} column (2.1 × 220 mm) as described for the Glu-C peptide mixture. Numbered peaks represent peptides submitted to sequencing and/or amino acid analysis.

RESULTS

Primary Structure of the Toad Lb-FABP. The amino acid sequence of several peptides obtained by digestion of the protein with trypsin, Glu-C, and cyanogen bromide was published elsewhere (*11*). To complete the primary structure determination, new fragments were generated by enzymatic digestion with proteases Glu-C and Lys-C (Figure 1A,B). On the basis of the amino acid composition of the resulting peptides, it was possible to select those corresponding to the toad Lb-FABP fragments whose amino acid sequences had not been determined earlier and also the overlapping peptides required. A map obtained after reverse-phase HPLC of the digestion products is shown in Figure 1A,B. Numbered peaks correspond to peptides sequenced and to those characterized by amino acid composition. The information obtained allowed completion of the full sequence except for the N-terminal residues (Figure 2). Bearing in mind that, according to amino acid determinations and already estab-

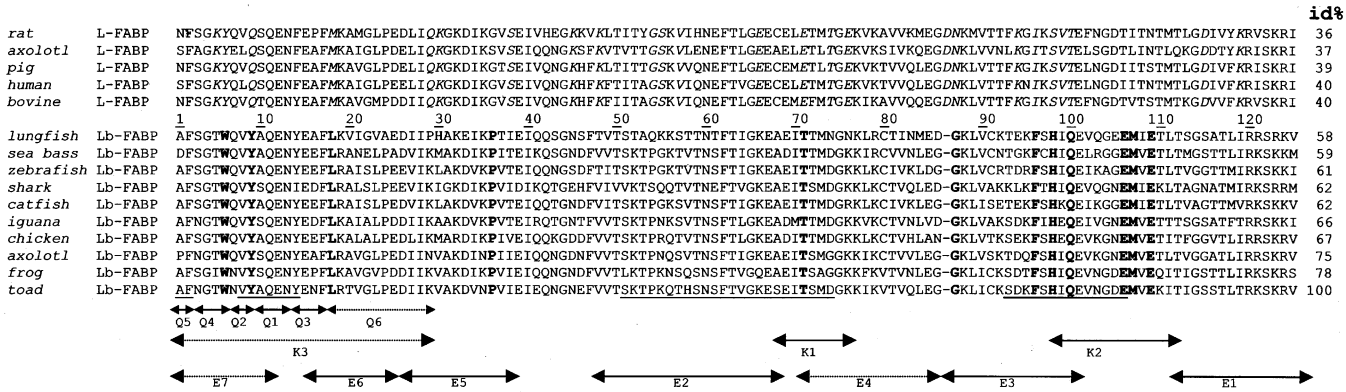

FIGURE 2: Primary structure of toad Lb-FABP and its sequence alignment with Lb-FABPs and L-FABPs. Peptide fragments are indicated by solid arrows when determined by sequencing, and by a dotted line arrow for those inferred on the basis of their amino acid analysis. Each peptide is labeled with a letter E for Glu-C digestion derived peptides, K for peptides obtained from Lys-C digestion, and Q for those generated by chymotryptic digestion−and a number that agrees with that of Figure 1. Numbers above the sequence indicate residue positions in the protein. Underlined residues correspond to the new sequence added to the previously determined fragments (*11*). The amino acid sequence of toad Lb-FABP was aligned with those of all known Lb-FABPs and L-FABPs. Identity percentages between each FABP and toad Lb-FABP are indicated after each amino acid sequence. Residues conserved in all Lb-FABPs and not in the L-FABPs are shown in bold and those conserved in all L-FABPs but not in Lb-FABP are displayed in italics.

lished sequences, tryptophan and tyrosine residues are found only in the N-terminal portion of toad Lb-FABP, the blocked N-terminal Lys-C peptide (K3) was identified and digested with chymotrypsin. The resulting peptides were isolated by reverse-phase HPLC (Figure 1C) and submitted to amino acid analysis and/or sequencing. One of them yielded negative results by Edman degradation (Q5), thus indicating a blocked α-amino group. Its amino acid composition Ala, Phe, showed, according to the chymotrypsin specificity, that Ala is the N-terminal residue.

The protein has 125 residues (Figure 2) and, on the basis of its amino acid sequence, the molecular mass was calculated as 13990 Da, considering an N-terminal acetyl group. This value is almost identical with that obtained by electrospray mass spectrometry (13987 ± 2 Da) (*11*). The calculated isoelectric point (6.98) agrees with that obtained experimentally (6.80) (*11*).

Evolutionary Relationships. The alignment of the amino acid sequence of toad Lb-FABP with L-FABPs isolated from the liver of rat, axolotl, pig, human, and bovine and with Lb-FABPs from lungfish, sea bass, zebrafish, shark, catfish, iguana, chicken, axolotl, and frog is shown in Figure 2. Identities between toad Lb-FABP and the other FABPs are indicated in the same figure. Toad Lb-FABP is more closely related to the other Lb-FABPs than to mammalian and axolotl L-FABPs. In addition, toad Lb-FABP conserves the 12 characteristic residues present in all Lb-FABPs but not in L-FABPs: Trp 6, Tyr 9, Leu 18, Pro 36, Thr 71, Gly 87, Phe 96, His 98, Gln 100, Glu 106, Met 107, and Glu 109 (Figure 2). In the evolutionary tree of vertebrate FABPs (Figure 3), toad Lb-FABP also appears to be closely related to the other Lb-FABPs.

Three-Dimensional Structure. Toad Lb-FABP presents the canonical fold characteristic of all the members of this protein family, a β-barrel containing 10 antiparallel β-strands and two α-helices. Figure 4A is a stereo diagram with the side chains that are present in all the Lb-FABPs and not in the L-FABPs (Figure 2). Eight out of the 12 conserved residues point to the lipid-binding cavity of the molecule and six cluster in the region spanning amino acids 96−109, which suggests that these side chains might be involved in the specific binding of a heretofore not identified specific ligand. Table 2 lists a series of members of the FABP family of known crystal structure in order of descending percentage of sequence identity with toad Lb-FABP. The overall rmsd between the equivalent α-carbons of toad Lb-FABP and those of the other FABPs is also shown in Table 2. Not surprisingly, L-FABP is the protein with the highest sequence identity and closest three-dimensional structure to Lb-FABP. Nevertheless, the calculated average rmsd value is significantly higher than those obtained for very closely related members in this protein family like, for example, the CRBPs (*62*) and indicative of significant structural and possibly functional differences between L-FABPs and Lb-FABPs.

Surface Electrostatic Potential. Figure 4B shows the electrostatic potential contours for toad Lb-FABP, on the left oriented as in Figure 4A and on the right rotated 180° about a central vertical axis. Notice in the model on the left that the interior of the binding cavity is found to be strongly negative with a ridge of positive potential visible on the molecular surface. The molecule viewed from the other side, i.e., rotated 180° about its vertical axis presents, on the other hand, a more irregular distribution of surface charges. Interestingly, the helix−turn−helix motif shows both negative and positive electrostatic potential surface (Figure 4B), the same as rat L-FABP, but in contrast with the other FABP types (*38*).

Fluorescent Fatty Acid-Binding Measurements. Toad Lb-FABP displayed high affinity for *cis*- and *trans*-parinaric acids; fluorescence intensity increased in a fatty acid concentration-dependent manner and was saturable. Figure 5 shows a representative binding experiment for each fluorescent fatty acid, performed under similar conditions to those used for the study of other FABPs (*10*, *13*, *18*, *22*, *23*, *27*, *28*). Upon titration of previously delipidated toad Lb-FABP with *cis*-parinaric (Figure 5A) or *trans*-parinaric acid (Figure 5B), saturation curves were obtained. Scatchard plots of these binding curves show that toad Lb-FABP can bind two *cis*-parinaric acid molecules but only one *trans*-parinaric acid molecule (Figure 5A,B). Toad Lb-FABP dissociation constants (K_D) for *cis*-parinaric acid are 35 ± 8 nM and 380 ± 34 nM for the primary and secondary binding

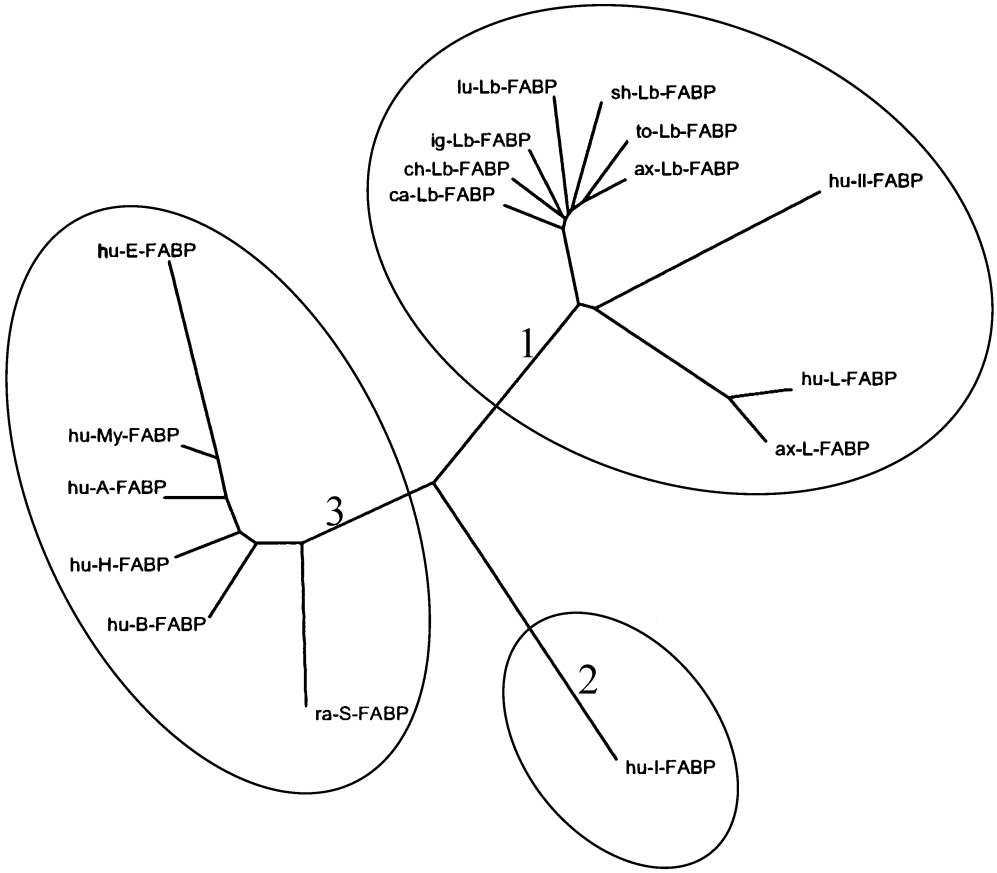

FIGURE 3: Evolutionary tree of the FABP family. Unrooted evolutionary tree based on a multiple sequence alignment of representative members of the Lb-FABPs and L-FABPs with the human or rat member of the rest of the FABP types. The tree was constructed with CLUSTAL W by the Neighbor Joining method and using the Kimura correction of distances.

sites, respectively, and that for *trans*-parinaric acid is 78 ± 17 nM (values represent mean ± SEM, $n = 3$).

Displacement of cis-Parinaric Acid by Fatty Acids and Other Ligands. To compare the affinity of toad Lb-FABP for fatty acids, fatty acyl-CoAs, lysophospholipids, prostaglandins, retinoids, and other ligands, *cis*-parinaric acid-displacement assays were performed (Table 3). Under similar experimental conditions to those used for the study of other FABPs (*10*, *13*, *18*, *22*, *23*, *27*, *28*), we found that the better fatty acid displacers were the mono- and polyunsaturated ones, specially those of 18-carbon atoms, with saturated fatty acids showing a low displacing capacity (Table 3). Such fatty acid-affinity pattern is similar to that of axolotl and lungfish Lb-FABPs but different from that of catfish Lb-FABP (*10*, *13*, *18*). Toad Lb-FABP has a broad ligand-binding specificity: in addition to fatty acids, several structurally different hydrophobic ligands displace *cis*-parinaric acid effectively (Table 3). The affinity of toad Lb-FABP for several of those ligands is similar to that for fatty acids: both saturated and unsaturated fatty acyl-CoAs, bilirubin, retinol, and bile salts (Table 3). Moreover, the affinity of toad Lb-FABP for lysophosphatidic acid, lysophospholipids containing different headgroups and retinoic acid is higher than that for fatty acids (Table 3). However, its affinity for prostaglandins is moderate and that for peroxisomal proliferators, bezafibrate and clofibrate is rather low.

Effect of Vesicle Concentration on AOFA Transfer from Lb-FABP to Membranes. Transfer of a hydrophobic ligand from a protein to a membrane can occur by different mechanisms. One possibility is aqueous diffusion where the rate-limiting step is the release of the fatty acid from the protein. In contrast, in the collisional mechanism the effective interaction between protein and membrane results in ligand transfer. To distinguish between these transfer mechanisms, AOFA transfer from toad Lb-FABP to model membranes was examined as a function of increasing membrane concentration. No change in the transfer rate is expected for a diffusional mechanism since the rate of ligand dissociation from the protein is independent of the acceptor, whereas for collisional transfer, the rate of ligand movement will increase as the number of protein−membrane collisions rises and hence as the acceptor membrane concentration increases. Figure 6A shows the results obtained when a constant concentration of toad Lb-FABP was mixed with increasing concentrations of EPC SUVs. Increasing the concentration of acceptor vesicles did not affect the transfer rate of 12AO from Lb-FABP. This result supports the hypothesis that AOFA transfer from Lb-FABP to acceptor membranes is occurring through an aqueous diffusion-mediated mechanism, quite similar to the effect observed for L-FABP in previous works (*29*, *30*) and as shown in the inset of Figure 6A. In addition, the average rate of 12AO transfer from Lb-FABP was more than 10 times faster than that from L-FABP (Figure 6A, inset) but quite similar to the value obtained for I-FABP (*33*).

Effect of Vesicle Charge on AOFA Transfer from Lb-FABP to Membranes. Changes in the surface charge density of the acceptor vesicles can also influence ligand transfer rates if

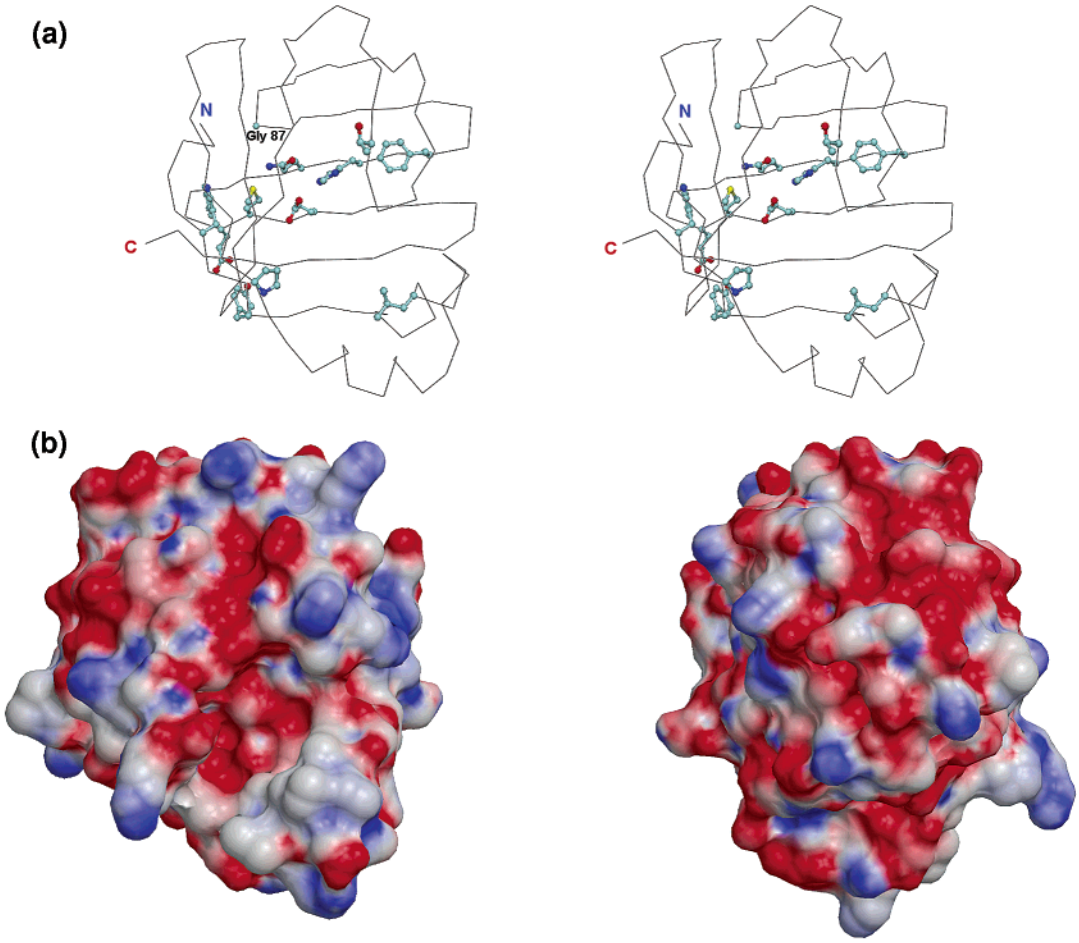

FIGURE 4: Three-dimensional structure of toad Lb-FABP. (A) Stereo representation of the crystal structure of toad Lb-FABP showing the side chains of the conserved amino acids in the family of the Lb-FABP that are not present in L-FABPs. The residues represented are Trp 6, Tyr 9, Leu 18, Pro 36, Thr 71, Gly 87, Phe 96, His 98, Gln 100, Glu 106, Met 107, and Glu 109. Notice that most of the conserved residues point to the lipid-binding cavity of the molecule. (B) Electrostatic potential contours for toad Lb-FABP. Blue is positive potential and red is negative. The left-hand picture shows the molecule oriented as in A and the right-hand picture displays the molecule rotated 180° around a central vertical axis so that what is seen is the "rear view" of the protein model.

Table 2: Comparison of the Amino Acid Sequence and Overall rmsd between Toad Lb-FABP and Other Members of the FABP Family in Order of Descending Sequence Identity[a]

FABP	identity (%)	Swiss Prot ID code	rmsd (Å)	PDB ID code	ref
rat holo-L-FABP	36.3	P02692	1.41	1LFO	*21*
rat apo-I-FABP	29.2	P02693	1.74	1IFB	*74*
mouse apo-A-FABP	27.8	P04117	1.63	1LIB	*75*
bovine holo My-FABP	26.2	P02690	1.55	1PMP	*76*
human holo H−FABP	26.1	P05413	1.63	1HMS	*77*
human holo B−FABP	24.7	O15540	1.64	1FDQ	*78*
human holo-E-FABP	18.6	Q01469	1.56	1B56	*79*

[a] rmsd between α-carbon atoms of toad Lb-FABP and the corresponding atoms of the other FABPs were calculated with the program TOP3D of the CCP4 package (*45*).

electrostatic interactions between donor protein and acceptor membranes are involved, whereas in the case of aqueous diffusion, the characteristics of the acceptor membrane are not expected to regulate the transfer rate. Figure 6B shows that 12AO transfer rate from Lb-FABP is essentially unaffected by the presence of negatively charged phospholipids (incorporation of 25 mol % PS or CL into EPC/NBD-PC acceptor membranes). The same behavior was observed for L-FABP (Figure 6B, inset) which is in agreement with previous works (*30*). These results further support the hypothesis that AOFA transfer of fatty acids from Lb-FABP occurs most likely via aqueous diffusion.

Effect of Ionic Strength on AOFA Transfer from FABPs to Membranes. The aqueous solubility of fatty acids is inversely related to the ionic strength of the solvent (*63*, *64*). Thus, the rate of transfer of AOFA from a binding protein through an aqueous space to an acceptor membrane is expected to decrease with the increase in salt concentration of the media. Lb-FABP shows a decrease in the transfer rate for 12AO to SUVs (Figure 6C) which is also observed for L-FABP (Figure 6C, inset) and fully agrees with previous findings for AOFA transfer from L-FABP to SUVs (*29*, *30*). This behavior was also observed for the transfer from donor SUVs to L-FABP (*37*), and is supportive of the hypothesis that the transfer takes place through an aqueous-phase intermediate. On the other hand, a salt-dependent increase for AOFA transfer from H-FABP to SUVs was suggested to be indicative of collisional interaction between H-FABP and SUVs during AOFA transfer (*31*, *32*). Moreover, the AOFA transfer rate from donor SUVs to I-FABP also showed an increase with ionic strength (*37*) which was understood to indicate that a mechanism different from an aqueous mediated one was taking place in AOFA transfer from zwitterionic SUVs to I-FABP.

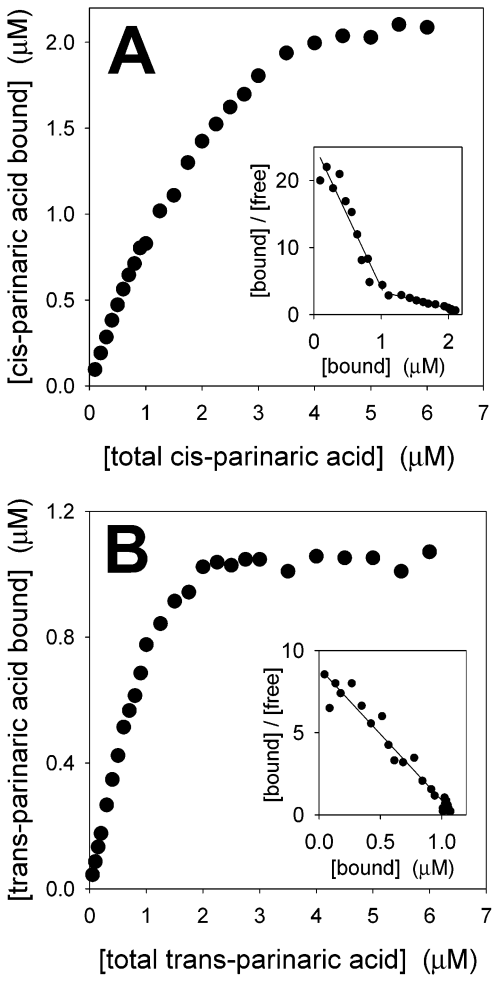

FIGURE 5: Titration curves for the binding of cis-parinaric and trans-parinaric acids to toad Lb-FABP. (A) Binding of cis-parinaric acid (0−6 μM) to delipidated toad Lb-FABP (1 μM) in 50 mM Tris-HCl (pH 7.4) was performed following the procedure of Nemecz et al. (*23*) as modified by Schroeder et al. (*73*). Inset, Scatchard plot of the titration. (B) Binding of trans-parinaric acid to toad Lb-FABP and the corresponding Scatchard plot (inset) were determined as in (A).

Table 3: Displacement of *cis*-Parinaric Acid from Toad Lb-FABP by Different Ligands

displacing ligand	displacement (%)[a]
palmitic acid	42 ± 3
stearic acid	44 ± 2
arachidic acid	31 ± 5
palmitoleic acid	56 ± 3
oleic acid	63 ± 1
linoleic acid	61 ± 5
linolenic acid	64 ± 4
arachidonic acid	60 ± 7
CoA	1± 2
palmitoyl-CoA	54 ± 2
stearoyl-CoA	56 ± 3
palmitoleoyl-CoA	53 ± 3
oleoyl-CoA	62 ± 5
linoleoyl-CoA	54 ± 6
lysophosphatidic acid	87 ± 3
lysophosphatidyl-choline	82 ± 6
lysophosphatidyl-inositol	81 ± 4
lysophosphatidyl-serine	84 ± 4
lysophosphatidyl-glycerol	79 ± 5
prostaglandin A_1	48 ± 2
prostaglandin E_1	44 ± 4
prostaglandin E_2	41 ± 3
prostaglandin J_2	43 ± 6
all-trans-retinol	50 ± 3
all-trans-retinal	53 ± 3
all-trans-retinoic acid	89 ± 5
9-*cis*-retinoic acid	83 ± 6
13-*cis*-retinoic acid	85 ± 4
bezafibrate	40 ± 2
clofibrate	48 ± 4
bilirubin	50 ± 9
bile salts	64 ± 3
palmitoyl-carnitine	35 ± 5

[a] Displacement is given as the percentage of *cis*-parinaric acid binding to toad Lb-FABP in the absence of the displacing ligand. Concentrations are 0.3 μM delipidated FABP, 1 μM *cis*-parinaric acid, and 3 μM displacing ligand. Values are means ± SD of three experiments.

DISCUSSION

According to the evolutionary tree (Figure 3), vertebrate FABPs belong to three branches: (i) liver and ileum FABPs, (ii) intestinal FABPs, and (iii) a complex branch including heart, brain, adipocyte, myelin, sperm, and epithelial FABPs and also the rest of the family members. Branch 1 is divided into three subgroups corresponding to Lb-FABPs, Il-FABPs, and L-FABPs including that of axolotl. These data agree with our previous trees resulting from the analysis of 51 (*6*) and 63 (*4*) family members from vertebrates and invertebrates. The evolutionary analysis, that takes into account the amino acid substitution rate of each FABP type, suggests that the common ancestor of the liver (i) and intestinal (ii) branch diverged from branch 3, approximately 1000 million years ago (*13*, *65*, Di Pietro and Santomé, unpublished results), while branches 1 and 2 diverged about 815 million years ago and Lb-FABP and L-FABP approximately 694 million years ago (*13*).

The sequence comparison of toad Lb-FABP with that of the already known members of Lb-FABP subfamilies indicates that it is more closely related to those of other amphibian proteins (frog and axolotl) (78 and 75% identity, respectively) than to those of reptiles (66%), birds (67%), and fish (58−62%) (Figure 2). These data agree with the evolutionary relationship between those species though the lowest value for fish is that of the lungfish Lb-FABP, a close relative of tetrapods (*18*). Nevertheless, the values of *cis*-parinaric acid displacement by fatty acids, fatty acyl-CoAs, lysophospholipids, prostaglandins, retinoids, and other ligands are quite similar for toad Lb-FABP and lungfish Lb-FABP (*18*) and less similar to those of axolotl Lb-FABP (*13*).

The overall rmsd between the equivalent α-carbons of toad Lb-FABP and those of FABPs belonging to other types (Table 2) are similar and agree with the values obtained when rat L-FABP is compared with the other FABPs (*21*), suggesting that functional specificity should not be based on gross structural differences. In addition, it is well-known that, despite the differences between the amino acid sequences of family members, their three-dimensional structures remain highly conserved (*3*). Therefore, it is not surprising to find a low correlation between the rmsd values and the corresponding FABP positions in the evolutionary tree (Figure 3). Despite the relatively low rmsd between the equivalent α-carbons of toad Lb-FABP and L-FABP and their sequence similarity, the conserved residues in each of these proteins are located in different molecular positions: while in toad Lb-FABP, 8 of the 12 Lb-FABPs characteristic

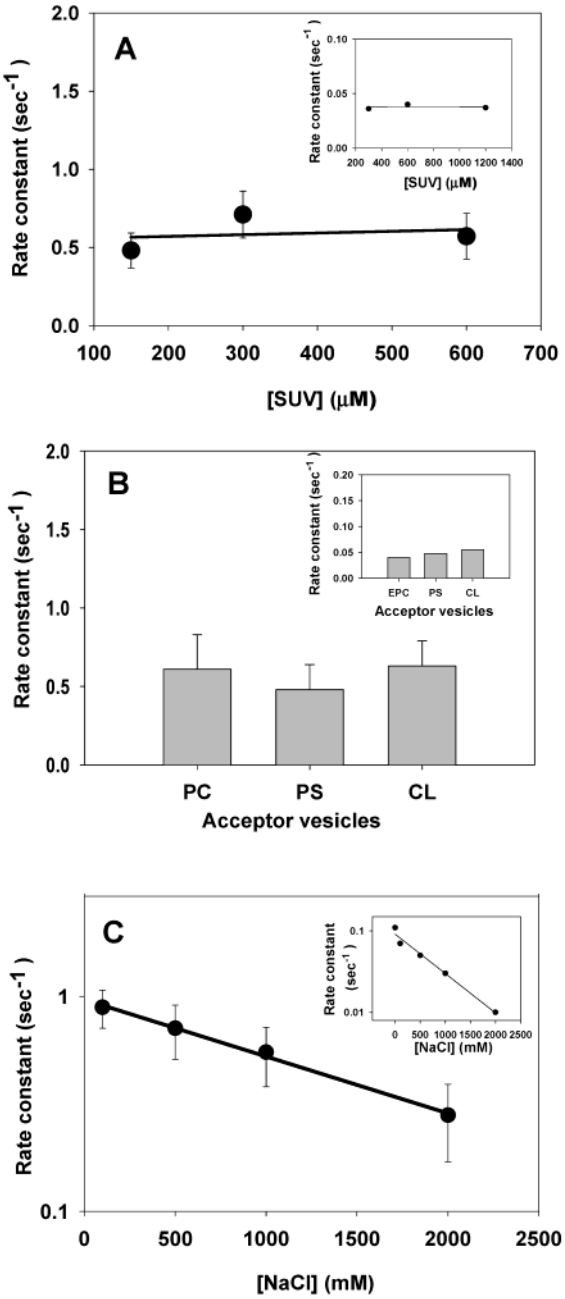

FIGURE 6: 12AO Transfer from Lb-FABP to model membranes. (A) Effect of acceptor membrane concentration on AOFA transfer from Lb-FABP. Transfer of 0.125 μM 12AO from 12.5 μM Lb-FABP to EPC/NBD-PC SUV. A single comparative experiment is shown in the Inset (0.5 μM 12AO from 5 μM L-FABP to EPC/NBD-PC SUV). (B) Effect of vesicle charge on AOFA transfer from FABP. Transfer of 0.125 μM 12AO from 12.5 μM Lb-FABP to 150 μM EPC/NBD-PC SUV containing 25 mol % of PS or CL. A single comparative experiment is shown in the inset (0.5 μM 12AO from 5 μM L-FABP to 300 μM EPC/NBD-PC SUV containing 25 mol % of PS or CL). (C) Effect of ionic strength on AOFA transfer from Lb-FABP. Transfer of 0.125 μM 12AO from 12.5 μM Lb-FABP to 150 μM EPC/NBD-PC SUV. A single comparative experiment is shown in the Inset (0.5 μM 12AO from 5 μM L-FABP to 300 μM EPC/NBD-PC SUV). The NaCl concentration of acceptor and donor were adjusted before mixing. Average transfer rates from three different experiments ± SD are shown.

residues have their side chains pointing to the binding cavity (Figure 4A), L-FABPs have 25 conserved residues not present in Lb-FABPs (Figure 2), most of them in clusters on the surface of the molecule.

L-FABP binds two fatty acid molecules, the carboxylate of one of them is internalized and that of the other is solvent-accessible (*21*). The picture is not so clear for Lb-FABPs, the catfish and chicken proteins bind only one molecule of ligand but Lb-FABP from other species, including toad, bind one or two ligand molecules, depending on its conformation (Figure 5) (*8*, *10*, *13*, *14*, *18*, *39*). Unfortunately, the toad Lb-FABP X-ray structure did not reveal the number and exact ligand(s) position. However, we found a residual electron density in the central cavity of the molecule, close to some of the Lb-FABP conserved residues (Figure 7). Interestingly, Gln 100 is present in CRBP I and II (*4*) and was shown to be directly hydrogen-bonded to the hydroxyl group of retinol (*62*). Taking into account that retinol is also a toad Lb-FABP ligand (Table 3), Gln 100 could interact with this ligand in a similar fashion. This position corresponds to an Arg in most FABP types and is involved in the carboxylate stabilization (*3*). His 98 could also interact with the ligand headgroup as suggested for His 108 of CRBP III and IV (*62*). Cys 91 also appears to interact with the hypothetical ligand, though it is not conserved in all Lb-FABPs (Figure 2) Cys 80 is very closely positioned (*18*) and could replace the Cys 91 function in those Lb-FABPs not having such a residue.

The above-mentioned residues and the other Lb-FABP conserved residues pointing to the ligand binding cavity (Figure 4A) may be related to the Lb-FABP affinity for several ligands, such as fatty acyl-CoAs, lysophospholipids, retinoids, bilirubin, and bile salts, that is similar to if not higher than that for fatty acids (Table 3). In contrast, the binding affinity of mammalian and axolotl L-FABP for long chain-fatty acids is higher than for other ligands (*4*, *13*, *26*, *27*). The apparent high affinity of Lb-FABP for retinoic acid deserves further investigation.

One distinctive biochemical characteristic of L-FABP is that the mechanism of fatty acid transfer to phospholipid membranes differs from that of the other FABP types (*29*−*37*, *66*). To address the role of the various FABPs in fatty acid transport to membranes, Storch et al. have systematically examined the way fluorescent anthroyloxy-labeled fatty acids are transferred from FABPs to egg phosphatidylcholine model membranes (*29*−*37*, *66*). In contrast with the other FABP types studied under the same assay conditions, fluorescent labeled-fatty acid transfer from L-FABP does not occur by collisional interaction with the membrane. L-FABP behavior is consistent with that of an aqueous diffusion mechanism involving the ligand release to the aqueous medium prior to membrane association (*29*, *30*, *66*). Moreover, the ligand transfer rate from L-FABP to membranes is the lowest reported for any FABP type and is 1 order of magnitude slower than I-FABP and 3 orders of magnitude slower than H-FABP and A-FABP (*66*). Using the same method, we have found that toad Lb-FABP shares with L-FABPs the aqueous diffusion mechanism for anthroyloxy-labeled fatty acid transfer to model membranes. However, the relative rate of toad Lb-FABP fluorescent fatty acid transfer is higher than those of rat L-FABP and similar to that of I-FABP which transfers the ligand by collisional interactions with the membrane.

Several reports have suggested that the helical domain of FABPs plays an important role in the mechanism and rate of fatty acid transfer to membranes (*32*, *33*, *36*). Using a

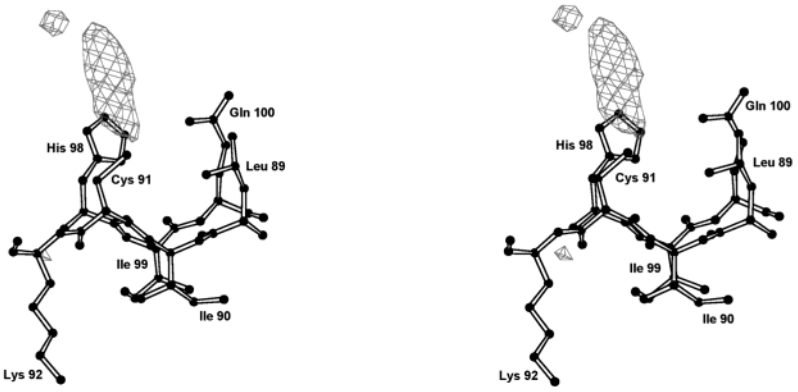

FIGURE 7: Stereo diagram representing the residual electron density present in the central cavity of the molecule. The amino acids in the figure are those that are closest to the peak. The Fobs − Fc map was calculated with the phases from the final protein model and contoured at a 3 σ level.

helix-less variant of I-FABP, it was proved that the α-helical region of I-FABP is involved in the protein−membrane interaction and appears to play a primary role in the collisional mechanism of fatty acid transfer from I-FABP to membranes (*33*, *67*). Moreover, employing a chimeric I/L-FABP (a protein with the "body" of I-FABP and the α-helical region of L-FABP), it has been recently observed that the α-helical region of L-FABP alters the rate and mechanism of fatty acid transfer from the chimeric FABP to model membranes compared to the wild-type proteins (Córsico, unpublished results). The analysis of the contribution of the α-helical domain of the Lb-FABP family regarding rates and transfer mechanisms could provide a better understanding of the possible differential role of these proteins as compared to L-FABP.

FABP types that transfer their ligand by a collisional mechanism share a solely positive electrostatic surface in the helical domain, important for the electrostatic interaction with the membrane (*38*). The presence of a both negative and positive surface potential in that molecular region was suggested to explain the different transfer mechanism of L-FABP (*38*). The electrostatic potential surface analysis of toad Lb-FABP (Figure 4B) shows that it has a both negative and positive surface potential at the level of the helix−turn−helix motif, similar to that of rat L-FABP, thus supporting the diffusional fatty acid transfer mechanism that both liver FABP types display. More subtle differences, possibly one or two residues, as shown for H-FABP and A-FABP (*32*, *68*), may account for the faster AOFA transfer rate of Lb-FABP in comparison with that of L-FABP.

At variance with the above, it was recently reported that L-FABP could interact with anionic membranes and concomitantly release the ligand (*69*, *70*). However, the L-FABP−membrane interaction was observed under different assay conditions, most notably using an extremely low ionic strength and no experiments were performed with other FABP types for comparison. Further experiments will be required to elucidate this apparent discrepancy regarding L-FABP. In any case, the L-FABP surface cationic residues Lys 30, Lys 35, and Lys 56, implicated in such effect (*70*), are not present in toad and other Lb-FABPs (Figure 2), which precludes this type of interaction for this group of proteins.

It has been suggested that the 1000 million year evolutionary process giving origin to at least 15 FABP types took place because each of them has specific functions in cellular metabolism (*1*, *2*, *4*, *65*, *66*). As mentioned above, despite the low sequence identity between different FABP types, their three-dimensional structures remain highly conserved (*3*), the functional specificity should therefore be based on the nature and position of side chains. It should be pointed out that the 12 Lb-FABP conserved residues were found in several species of fish and amphibians as well as in one reptile and one bird, suggesting their relevance in the biological activity of this protein. The eight side chains pointing to the central cavity are possibly related to the ligand specificity. On the other hand, the L-FABP 25 conserved residues are located in positions different from those of Lb-FABP, with the exception of Tyr 6, Ile 97, Ser 99, and Thr 101 which are in the position of Lb-FABP residues Trp 6, Phe 96, His 98, and Gln 100, respectively (Figure 2). Most of the L-FABP conserved residues are located on the surface thus suggesting that they may be involved in protein−protein interactions. Interestingly, such L-FABP−protein interactions were elegantly reported by Wolfrum et al. (*71*) for peroxisome proliferator-activated receptors α and γ and by Lawrence et al. (*72*) for an unidentified 33-kDa nuclear protein.

The coexpression of Lb-FABP and L-FABP in axolotl liver (*13*) suggests that they should have distinctive functional properties and this is strongly supported by the differences discussed here: amino acid sequence, location and nature of conserved residues, ligand binding preferences, and rate of transfer of fatty acids to membranes.

ACKNOWLEDGMENT

We acknowledge S. B. Linskens and E. V. Dacci for amino acid analysis and sequence determination.

REFERENCES

1. Matarese, V., Stone, R. L., Waggoner, D. W., and Bernlohr, D. A. (1989) Intracellular fatty acid trafficking and the role of cytosolic lipid binding proteins. *Prog. Lipid Res. 28*, 245−272.
2. Veerkamp, J. H., Peeters, R. A., and Maatman, R. G. H. J. (1991) Structural and functional features of different types of cytoplasmatic fatty acid-binding proteins. *Biochim. Biophys. Acta 1081*, 1−24.
3. Banaszak, L., Winter, N., Xu, Z., Bernlohr, D. A., Cowan, S., and Alwyn Jones, T. (1994) Lipid-binding proteins: a family of fatty acid and retinoid transport proteins. *Adv. Protein Chem. 45*, 89−115.
4. Santomé, J. A., Di Pietro, S. M., Cavagnari, B. M., Córdoba, O. L., and Dell'Angelica, E. C. (1998) Fatty acid-binding proteins.

Chronological description and discussion of hypotheses involving their molecular evolution. *Trends Comp. Biochem. Physiol. 4*, 23−38.
5. Ceciliani, F., Monaco, H. L., Ronchi, S., Faotto, L., and Spadon, P. (1994) The primary structure of a basic (pI 9.0) fatty acid binding protein from liver of *Gallus domesticus*. *Comp. Biochem. Physiol. 109B*, 261−271.
6. Schleicher, C. H., Córdoba, O. L., Santomé, J. A., and Dell'Angelica, E. C. (1995) Molecular evolution of the multigene family of intracellular lipid-binding proteins. *Biochem. Mol. Biol. Int. 36*, 1117−1125.
7. Scapin, G., Spadon, P., Pengo, L., Mammi, M., Zanotti, G., and Monaco H. L. (1988) Chicken liver basic fatty acid-binding protein (pI = 9.0). Purification, crystallization and preliminary X-ray data. *FEBS Lett. 240*, 196−200.
8. Schievano, E., Quarzago, D., Spadon, P., Monaco, H. L., Zanotti, G., and Peggion, E. (1994) Conformational and binding properties of chicken liver basic fatty acid-binding protein in solution. *Biopolymers 34*, 879−887.
9. Di Pietro, S. M., Dell'Angelica, E. C., Schleicher, C. H., and Santomé, J. A. (1996) Purification and structural characterization of a fatty acid-binding protein from the liver of the catfish *Rhamdia sapo*. *Comp. Biochem. Physiol. 113B*, 503−509.
10. Di Pietro, S. M., Dell'Angelica, E. C., Veerkamp, J. H., Sterin-Speziale, N., and Santomé, J. A. (1997) Amino acid sequence, binding properties and evolutionary relationships of the basic liver fatty acid-binding protein from the catfish *Rhamdia sapo*. *Eur. J. Biochem. 249*, 510−517.
11. Schleicher, C. H., and Santomé, J. A. (1996) Purification, characterization, and partial amino acid sequencing of an amphibian liver fatty acid binding protein. *Biochem. Cell. Biol. 74*, 109−115.
12. Córdoba, O L., Sánchez, E. I., Veerkamp, J. H., and Santomé, J. A. (1998) Presence of intestinal, liver and heart/adipocyte fatty acid-binding protein types in the liver of a Chimaera fish. *Int. J. Biochem. Cell. Biol. 30*, 1403−1413.
13. Di Pietro, S. M., Veerkamp, J. H., and Santomé, J. A. (1999) Isolation, amino acid sequencing and binding properties of two fatty acid-binding proteins from axolotl (*Ambistoma mexicanum)* liver. Evolutionary relationship. *Eur. J. Biochem. 259*, 27−134.
14. Córdoba, O. L., Sánchez, E. I., and Santomé, J. A. (1999) The main fatty acid binding protein in the liver of the shark (*Halaetunus bivius*) belongs to the liver basic type. Isolation, amino acid sequence determination and characterization. *Eur. J. Biochem. 265*, 832−838.
15. Baba, K., Abe, T. K., Tsunasawa, S., and Odani, S. (1999) Characterization and primary structure of a fatty acid-binding protein and its isoforms from the liver of the amphibian, *Rana catesbeiana*. *J. Biochem. 125*, 115−122.
16. Denovan-Wright, E. M., Pierce, M., Sharma, M. K., and Wright, J. M. (2000) cDNA sequence and tissue-specific expression of a basic liver-type fatty acid binding protein in adult zebrafish (Danio rerio). *Biochim. Biophys. Acta 1492*, 227−32.
17. Odani, S., Baba, K., Tsuchida, Y., Aoyagi, Y., Wakui, S., and Takahashi, Y. (2001) Hepatic fatty acid-binding proteins of a teleost, *Lateolabrax japonicus*. The primary structures and location of a disulfide bond. *J. Biochem. 129*, 69−76.
18. Di Pietro, S. M., and Santomé, J. A. (2001) Structural and biochemical characterization of the lungfish (*Lepidosiren paradoxa*) liver basic fatty acid-binding protein. *Arch. Biochem. Biophys. 388*, 81−90.
19. Haunerland, N., Jagschies, G., Schulenberg, H., and Spener, F. (1984) Fatty acid-binding proteins. Occurrence of two fatty acid-binding proteins in bovine liver cytosol and their binding of fatty acids, cholesterol, and other lipophilic ligands. *Hoppe-Seyler's Z. Physiol. Chem. 365*, 365−376.
20. Cistola, K. P., Sachettini, J. C., Banaszak, L. J., Walsh, M. T., and Gordon, J. Y. (1989) Fatty acid interactions with rat intestinal an liver fatty acid-binding proteins expresed in *Escherichia coli*. A comparative ^{13}C NMR study. *J. Biol. Chem. 264*, 2700−2710.
21. Thompson, J., Winter, N., Terwey, D., Bratt, J., and Banaszak, L. (1997) The crystal structure of the liver fatty acid-binding protein. A complex with two bound oleates. *J. Biol. Chem. 272*, 7140−7150.
22. Frolov, A., Cho, T. H., Murphy, E. J., and Schroeder, F. (1997) Isoforms of rat liver fatty acid-binding protein differ in structure and affinity for fatty acids and fatty acyl CoAs. *Biochemistry 36*, 6545−6555.
23. Nemecz, G., Hubbell, T., Jefferson, J. R., Lowe, J. B., and Schroeder, F. (1991) Interaction of fatty acids with recombinant rat intestinal and liver fatty acid-binding proteins. *Arch. Biochem. Biophys. 286*, 300−309.
24. Richieri, G. V., Ogata, R. T., and Kleinfeld, A. M. (1994) Equilibrium constants for the binding of fatty acids with fatty acid-binding proteins from adipocyte, intestine, heart, and liver measure with the fluorescent probe ADIFAB. *J. Biol. Chem. 269*, 23918−23930.
25. Veerkamp, J. H., van Kuppevelt, T. H. M. S. M., Maatman, R. G. H. J., and Prinsen, C. F. M. (1993) Structural and functional aspects of cytosolic fatty acid-binding proteins. *Prostaglandins Leukot. Essent. Fatty Acids 49*, 887−906.
26. Glatz, J. F. C., and van der Vusse, G. J. (1996) Cellular fatty acid-binding proteins: their function and physiological significance. *Prog. Lipid Res. 35*, 243−282.
27. Di Pietro, S. M., and Santomé, J. A. (2000) Isolation, characterization and binding proterties of two rat liver fatty acid-binding protein isoforms, *Biochim. Biophys. Acta 1478*, 186−200.
28. Jolly, C. A., Hubbell, T., Behnke, W. D., and Schroeder, F. (1997) Fatty acid binding protein: stimulation of microsomal phosphatidic acid formation, *Arch. Biochem. Biophys. 341*, 112−121.
29. Kim, H. H., and Storch, J. (1992) Free fatty acid transfer from rat liver fatty acid binding protein to phospholipid vesicles. Effect of ligand and solution properties. *J. Biol. Chem. 267*, 77−82.
30. Hsu, K. T., and Storch, J. (1996) Fatty acid transfer from liver and intestinal fatty acid-binding proteins to membranes occurs by different mechanisms. *J. Biol. Chem. 271*, 13317−13323.
31. Kim, H. H., and Storch, J. (1992) Mechanism of free fatty acid transfer from rat heart fatty acid-binding protein to phospholipid membranes. Evidence for a collisional process. *J. Biol. Chem. 267*, 20051−20056.
32. Herr, F. M., Aronson, J., and Stoch, J. (1996) Role of portal region lysine residues in electrostatic Interactions between heart fatty acid-binding protein and phospholipid membranes. *Biochemistry 35*, 1296−1303.
33. Córsico, B., Cistola, D. P., Frieden, C., and Storch, J. (1998) The helical domain of intestinal fatty acid binding protein is critical for collisional transfer of fatty acids to phospholipid membranes. *Proc. Natl. Acad. Sci. U.S.A. 95*, 12174−12178.
34. Storch, J., and Thumser, A. E. (2000) The fatty acid transport function of fatty acid-binding proteins. *Biochim. Biophys. Acta 1486*, 28−44.
35. Thumser, A. E., Tsai, J., and Storch, J (2001) Collision-mediated transfer of long-chain fatty acids by neural tissue fatty acid-binding proteins (FABP): studies with fluorescent analogues. *J. Mol. Neurosci. 16*, 143−157.
36. Liou, H. L., Kahn, P. C., and Storch, J. (2002) Role of helical domain in fatty acid transfer from adipocyte and heart fatty acid-binding proteins to membranes. *J. Biol. Chem. 277*, 1806−1815.
37. Thumser, E. A., and Storch, J. (2000) Liver and intestinal fatty acid-binding proteins obtain fatty acids from phospholipid membranes by different mechanisms. *J. Lipid Res. 41*, 647−656.
38. LiCata, V. J., and Bernlohr, D. A. (1998) Surface properties of adipocyte Lipid-binding protein: Response to lipid binding, and comparison with homologous proteins. *PROTEINS: Struct. Funct. Genet. 33*, 577−589.
39. Beringhelli, T., Goldoni, L., Capaldi, S., Bossi, A., Perduca, M., and Monaco, H. L. (2001) Interaction of chicken liver basic fatty acid-binding protein with fatty acids: A ^{13}C NMR and fluorescence study. *Biochemistry 40*, 12604−12611.
40. Di Pietro, S. M., Perduca, M., Santomé, J. A., and Monaco, H. L. (2001) Crystallization and preliminary X-ray study of two liver basic fatty acid binding proteins. *Acta Cryst. D57*, 1903−1905.
41. Glatz, J. F. C., and Veerkamp, J. H. (1983) A radiochemical procedure for the assay of fatty acid binding proteins. *Anal. Biochem. 132*, 89−95.
42. Bligh, E., and Dyer, N. (1959) A rapid method of total lipid extraction and purification. *Comp. Biochem. Physiol. 37*, 9−17.
43. Henschen A. (1986) in *Advanced Method in Protein Microsequence Analysis* (Wittman-Liebold, B., Salnikow, J., and Erdmann, V. A., Eds.) pp 244−255, Springer-Verlag, NY.
44. Leslie, A. G. W. (1992) Recent changes to the MOSFLM package for processing film and image plate data. *Jnt. CCP4/ESF-EACMB Newslett. Protein Crystallogr. 26*.
45. Collaborative Computational Project Number 4 (1994) *Acta Crystallogr. D50*, 760−767.
46. Navaza, J. (1994) AMoRe: an automated package for molecular replacement, *Acta Crystallogr. A50*, 157−163.

47. Tronrud, D. E., Ten Eyck, L. F., and Matthews, B. W. (1987) An efficient general-purpose least-squares refinement program for macromolecular structures. *Acta Crystallogr. A43*, 489−501.
48. Jones, T. A., Zou, J. Y., Cowan, S. W., and Kjeldgaard, M. (1991) Improved methods for the building of protein models in electron density maps and the location of errors in these models. *Acta Crystallogr. A47*, 110−119.
49. Laskowski, R. A., MacArthur, M. W., Moss, D. S., and Thornton, J. M. (1993) PROCHECK: a program to check the stereochemical quality of protein structures. *J. Appl. Crystallogr. 26*, 283−291.
50. Sanner, M. F., Olson, A. J., and Spehner, J. C. (1995) Fast and robust computation of molecular surfaces. *ACM 11th Symp. Comput. Geom. Vancouver B. C. Canada*, C6−C7.
51. Sanner, M. F., Olson, A. J., and Spehner, J. C. (1996) Reduced Surface: an efficient way to compute molecular surfaces. *Biopolymers 38*, 305−320.
52. Brunger, A. T., Adams, P. D., Clore, G. M., DeLano, W. L., Gros, P., Grosse-Kunstleve, R. W., Jiang, J. S., Kuszewski, J., Nilges, N., Pannu, N. S., Read, R. J., Rice, L. M., Simonson, T., and Warren, G. L. (1998) Crystallography and NMR system (CNS): A new software system for macromolecular structure determination. *Acta Crystallogr. D54*, 905−921.
53. Bashford, D., and Gerwert, K. (1992) Electrostatic calculations of the pK_a values of ionizable groups in bacteriorhodopsin. *J. Mol. Biol. 224*, 473−486.
54. Bashford, D. (1997) An object-oriented programming suite for electrostatic effects in biological molecules in scientific computing in object-oriented parallel environments. *Lecture Notes Comput. Sci. 1343*, 233−240.
55. Tyagi, S. C., and Simon, S. R. (1991) Parinaric acids as probes of binding domains in neutrophil elastase. *J. Biol. Chem. 266*, 15185−15191.
56. Huang, C., and Thompson, T. E. (1974) Preparation of homogeneous, single-walled phosphatidylcholine vesicles. *Method Enzymol. 32*, 485−489.
57. Storch, J., and Kleinfeld, A. M. (1986) Transfer of long-chain fluorescent free fatty acids between unilamellar vesicles. *Biochemistry 25*, 1717−1726.
58. Xu, Z., Buelt, M. K., Banaszak, L. J., and Bernlohr, D. A. (1991) Expression, purification, and crystallization of the adipocyte lipid binding protein. *J. Biol. Chem. 266*, 14367−14370.
59. Massey, J. B., Bick, D. H., and Pownall, H. J. (1997) Spontaneous transfer of monoacyl amphiphiles between lipid and protein surfaces. *Biophys. J. 72*, 1732−1734.
60. Storch, J., and Bass, N. M. (1990) Transfer of fluorescent fatty acids from liver and heart fatty acid-binding proteins to model membranes. *J. Biol. Chem. 265*, 7827−7831.
61. Roseman, M. A., and Thompson, T. E. (1980) Mechanism of the spontaneous transfer of phospholipids between bilayers. *Biochemistry 19*, 439−444.
62. Folli, C., Calderone, V., Ramazzina, I., Zanotti, G., and Berni, R. (2002) Ligand binding and structural analysis of a human putative cellular retinol-binding protein. *J. Biol. Chem. 277*, 41970−41977.
63. Tanford, C. (1980) *The Hydrophobic Effect: Formation of Micelles and Biological Membranes*, Wiley-Interscience, New York.
64. Charlton, S. C., and Smith, L. C. (1982) Kynetics of transfer of pyrene and rac-1-oleoyl-2-[4-(3-pyrenyl) butanoyl] glycerol between human plasma lipoproteins. *Biochemistry 21*, 4023−4030.
65. Chan, L., Wei, C. F., Li, W. H., Yang, C. Y., Ratner, P., Pownall, H., Gotto, A. M., and Smith, L. C. (1985) Human liver fatty acid binding protein cDNA and amino acid sequence. Functional and evolutionary implications. *J. Biol. Chem. 260*, 2629−2632.
66. Storch, J., Herr, F. M., Hsu, K. T., Kim, H. K., Liou, H. L., and Smith, E. R. (1996) The role of membranes and intracellular binding proteins in cytoplasmic transport of hydrophobic molecules: fatty acid-binding proteins. *Comp. Biochem. Physiol. 115B*, 333−339.
67. Wu, F., Córsico, B., Flach, C. R., Cistola, D., Storch, J., and Mendelsohn, R. (2001) Deletion of the helical motif in the intestinal fatty acid-binding protein reduces its interactions with membrane monolayers: Brewster angle microscopy, IR reflection−absorption spectroscopy and surface pressure studies. *Biochemistry 40*, 1976−1983
68. Liou, H. L., and Storch, J. (2001) Role of surface lysine residues of adipocyte fatty acid-binding protein in fatty acid transfer to phospholipid vesicles. *Biochemistry 40*, 6475−6485.
69. Davies, J. K., Thumser, A. E. A., and Wilton, D. C. (1999) Binding of recombinant rat liver fatty acid-binding protein to small anionic phopholipid vesicles results in ligand release: a model for interfacial binding and fatty acid targeting. *Biochemistry 38*, 16932−16940.
70. Davies, J. K., Hagan, R. M., and Wilton, D. C. (2002) Effect of charge reversal mutations on the ligand- and membrane-binding properties of liver fatty acid-binding protein. *J. Biol. Chem. 277*, 48395−48402.
71. Wolfrum, C., Borrmann, C. M., Borchers, T., and Spener, F. (2001) Fatty acids and hypolipidemic drugs regulate peroxisome proliferator-activated receptors alpha−and gamma-mediated gene expression via liver fatty acid binding protein: a signaling path to the nucleus. *Proc. Natl. Acad. Sci. U.S.A. 98*, 2323−2328.
72. Lawrence, J. W., Kroll, D. J., and Eacho, P. I. (2000) Ligand-dependent interaction of hepatic fatty acid-binding protein with the nucleus. *J. Lipid Res. 41*, 1390−1401.
73. Schroeder, F., Myers-Payne, S. C., Billheimer, J. T., and Wood, W. G. (1995) Probing the ligand binding sites of fatty acid and sterol carrier proteins: effects of ethanol. *Biochemistry 34*, 11919−11927.
74. Sacchettini, J. C., Gordon, J. I., and Banaszak, L. J. (1989) Refined apoprotein structure of rat intestinal fatty acid binding protein produced in *Escherichia coli*. *Proc. Natl. Acad. Sci. U.S.A. 86*, 7736−7740.
75. Xu, Z., Bernlohr, D. A., and Banaszak, L. J. (1993) The adipocyte lipid-binding protein at 1.6-A resolution. Crystal structures of the apoprotein and with bound saturated and unsaturated fatty acids. *J. Biol. Chem. 268*, 7874−7884.
76. Cowan, S. W., Newcomer, M. E., and Jones, T. A. (1993) Crystallographic studies on a family of cellular lipophilic transport proteins. Refinement of P2 myelin protein and the structure determination and refinement of cellular retinol-binding protein in complex with all-trans-retinol. *J. Mol. Biol. 230*, 1225−1246.
77. Young, A. C., Scapin, G., Kromminga, A., Patel, S. B., Veerkamp, J. H., and Sacchettini, J. C. (1994) Structural studies on human muscle fatty acid binding protein at 1.4 A resolution: binding interactions with three C18 fatty acids. *Structure 2*, 523−534.
78. Balendiran, G. K., Schnutgen, F., Scapin, G., Borchers, T., Xhong, N., Lim, K., Godbout, R., Spener, F., and Sacchettini, J. C. (2000) Crystal structure and thermodynamic analysis of human brain fatty acid binding protein. *J. Biol. Chem. 275*, 27045−27054.
79. Hohoff, C., Borchers, T., Rustow, B., Spener, F., and Van Tilbeurgh, H. (1999) Expression, purification and crystal structure determination of recombinant human epidermal-type fatty acid-binding protein. *Biochemistry 38*, 12229−12239.

BI034213N